

Information flow and nontrivial collective behavior in chaotic-coupled-map lattices

Ming-Chung Ho* and Fu-Chi Shin

Department of Physics, National Kaohsiung Normal University, Kaohsiung, Taiwan

(Received 13 September 2002; revised manuscript received 25 February 2003; published 22 May 2003)

This work quantitatively demonstrates a nontrivial collective behavior, which depends on the coupling strength in chaotic-coupled-map lattices, using the interdependence measure emerging from a local unit. The amount of information flow which flows from the instantaneous mean field to a local map has been investigated using the time-delayed mutual information. Interestingly, the collective system's behavior is found to be associated with the amount of information flow. As mentioned above, both methods can effectively display the nontrivial collective behavior and the amount of information flow.

DOI: 10.1103/PhysRevE.67.056214

PACS number(s): 05.45.Ra, 02.50.-r

I. INTRODUCTION

Chaotic-coupled-map lattices are highly complex and exhibit various phenomena. They are therefore often used as typical models for investigating the characteristics of real spatiotemporal systems, such as the phenomena of cooperation in many extended chaotic dynamical systems [1]. Recently, many researchers have sought to understand the emergence of nontrivial collective behavior (NTCB) in chaotic-coupled-map lattices [2,3]. In particular, Cisneros *et al.* presented an important advance in understanding NTCB [3] with reference to coupled maps, such as regular Euclidean lattices [2,4], one-dimensional locally coupled-map lattices [5], fractal geometries [6], and globally coupled-map networks [7–10]. This study characterizes NTCB using the interdependence measure emerging from a local unit [11], and the amount of information flow which flows from the instantaneous mean field h_n to a local map x_{n+1}^i using the time-delayed mutual information [12]. The relationship between NTCB and information flow is examined. Both methods can effectively quantify NTCB and the amount of information flow, respectively.

The rest of this paper is organized as follows. Section II presents various models of chaotic coupled map lattices. Section III then describes a measure used to quantify the collective dynamics of a system. Section IV investigates the relationship between nontrivial collective behavior and the amount of information flow. Section V draws conclusions.

II. MODELS OF CHAOTIC-COUPLED-MAP LATTICES

This section presents four models of chaotic-coupled-map lattices, which are used throughout this paper. The first two examples refer to global coupled-map systems, defined as

$$x_{n+1}^i = (1 - \varepsilon)f_i(x_n^i) + \frac{\varepsilon}{N} \sum_{j=1}^N f_j(x_n^j), \quad (1)$$

where the function $f_i(x_n^i)$ denotes the local dynamics of element i and ε represents the coupling strength. The first example is of the homogeneous, globally coupled-map sys-

tems, of which all elements exhibit the same local function, such that $f_i(x_n^i) = f(x_n^i)$. Local dynamics are achieved using the logarithmic map $f(x) = b + \ln|x|$, where b is a real parameter. This map differs from the standard classes of universality of unimodal or bounded maps. Specifically, the behavior of this map does not have periodic windows or separated chaotic bands in the interval $b \in [-1, 1]$. In the second example, heterogeneity of the local dynamics in Eq. (1) is introduced with $f_i(x_n^i) = b_i + \ln|x_n^i|$, where the parameters b_i are distributed in $[-1, 1]$. The third example is of the one-dimensional, homogeneous, diffusively coupled logarithmic map lattices, given by

$$x_{n+1}^i = (1 - \varepsilon)f(x_n^i) + \frac{\varepsilon}{2}[f(x_n^{i-1}) + f(x_n^{i+1})], \quad (2)$$

where the boundary conditions in Eq. (2) are periodic. The three above-mentioned examples are the same as in Ref. [3], and an additional example is presented to demonstrate the advantages of the proposed methods. The form of the final example is the same as that of Eq. (1); however, the local dynamic is replaced by a tent map $f(x) = a(1 - |x|)$, which also exhibits nontrivial collective behavior [13]. Setting $a = 1.5$ makes this map chaotic. The collective system behavior is defined as

$$A_n = \frac{1}{N} \sum_{j=1}^N x_n^j, \quad (3)$$

and the instantaneous mean field is given by

$$h_n = \frac{1}{N} \sum_{j=1}^N f_j(x_n^j). \quad (4)$$

The following section uses the above four models to demonstrate how the interdependence measure quantitatively describes the nontrivial collective behavior.

III. METHOD OF INTERDEPENDENCE

This section introduces a method for quantifying the collective behavior of a system. First, the concept of interdependence measure is briefly described [11]. Assume that two simultaneously measured, univariate time series exist, from

*Electronic address: ho@mail.phy.nknu.edu.tw

which m -dimensional delay vectors $\mathbf{x}_n = (x_n, \dots, x_{n-m+1})$ and $\mathbf{y}_n = (y_n, \dots, y_{n-m+1})$, $n = 1, \dots, N$ can be constructed. Then, let $l_{n,j}$, $j = 1, \dots, k$ denote the time indices of the k closest neighbors of \mathbf{x}_n . For each \mathbf{x}_n , the squared mean Euclidean distance to its k neighbors is defined as

$$R_n^{(k)}(\mathbf{X}) = \frac{1}{k} \sum_{j=1}^k (\mathbf{x}_n - \mathbf{x}_{l_{n,j}})^2. \quad (5)$$

The corresponding time indices of the k closest neighbors of \mathbf{y}_n are termed $s_{n,j}$. Then the \mathbf{Y} -conditioned squared mean Euclidean distance is defined by

$$R_n^{(k)}(\mathbf{X}|\mathbf{Y}) = \frac{1}{k} \sum_{j=1}^k (\mathbf{x}_n - \mathbf{x}_{s_{n,j}})^2. \quad (6)$$

If the systems are strongly correlated, then $R_n^{(k)}(\mathbf{X}|\mathbf{Y}) \approx R_n^{(k)}(\mathbf{X})$ is expected, while if they are independent, then $R_n^{(k)}(\mathbf{X}|\mathbf{Y}) \gg R_n^{(k)}(\mathbf{X})$ is expected. Accordingly, a measure of dependence such as

$$S^{(k)}(\mathbf{X}|\mathbf{Y}) = \frac{1}{N} \sum_{n=1}^N \frac{R_n^{(k)}(\mathbf{X})}{R_n^{(k)}(\mathbf{X}|\mathbf{Y})} \quad (7)$$

can be defined, which takes values from almost 0 for independent systems to 1 for strongly dependent and identical systems. A measure with similar properties is

$$H^{(k)}(\mathbf{X}|\mathbf{Y}) = \frac{1}{N} \sum_{n=1}^N \ln \frac{R_n(\mathbf{X})}{R_n^{(k)}(\mathbf{X}|\mathbf{Y})}, \quad (8)$$

where $R_n(\mathbf{X}) = (N-1)^{-1} \sum_{j \neq n} (\mathbf{x}_n - \mathbf{x}_j)^2$. H differs from S only in the use of the conditional distance rather than the mean distance to all other points and the use of the natural logarithm. Both quantities have been proven to be useful in real data applications and simple toy models. $H^{(k)}(\mathbf{X}|\mathbf{Y})$ is considered useful here, since it is sensitive to weak dependencies. $H^{(k)}(\mathbf{X}|\mathbf{Y})$ is zero if \mathbf{X} and \mathbf{Y} are completely independent, and is positive if nearness in \mathbf{Y} also implies nearness in \mathbf{X} for equal time partners. For identical systems, $H^{(k)}(\mathbf{X}|\mathbf{Y})$ is just a high positive value, but $S^{(k)}(\mathbf{X}|\mathbf{Y}) = 1$. Therefore, $S^{(k)}(\mathbf{X}|\mathbf{Y})$ is used as an auxiliary measure to examine the synchronized state. $H^{(k)}(\mathbf{X}|\mathbf{Y})$ would be negative if close pairs in \mathbf{Y} were to correspond mainly to distant pairs in \mathbf{X} . This situation is very unlikely but not impossible. The following section demonstrates the nontrivial collective behavior of the three models introduced above by applying the interdependence measure H to both the collective behavior A_n and a local map x_n^i .

A. Homogeneous, globally coupled logarithmic map lattices

First, the homogeneous, globally coupled logarithmic map lattices are investigated. Figure 1(a) presents the bifurcation diagram of the average state A_n as a function of coupling strength ε . The return maps of A_n are also demonstrated for different couplings in Fig. 2. However, Fig. 1(a) indicates that different collective behaviors emerge as a function of the

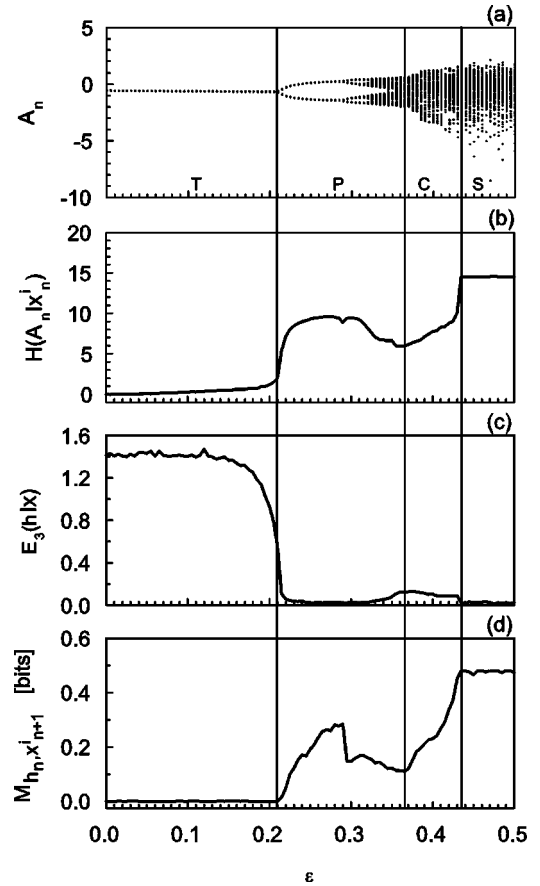


FIG. 1. (a) Bifurcation diagram A_n vs ε for homogeneous, globally coupled logarithmic maps with $b=0$ and system size $N = 10^4$. Four different phases are observed: turbulent, T ; periodic, P ; chaos bands, C ; and synchronized, S . (b) $H(A_n|x_n^i)$ vs ε for this system. (c) Average information flow M_{h_n, x_{n+1}^i} from h_n to x_{n+1}^i , with $r=0.2$.

coupling strength ε . A turbulent phase T is observed in Fig. 2(a), where A_n manifests as a fixed point, follows the standard statistical behavior of uncorrelated disordered variables; collective periodic states P [Fig. 2(b)]; collective chaotic bands C [Fig. 2(c)]; and chaotic synchronization S [Fig. 2(d)]. Next, the interdependence measure is then used to describe different behaviors for different coupling strengths in Fig. 1(a). The system size is $N = 10\,000$ and the local parameter b is fixed at zero for all maps. For each value of ε , the initial conditions are random, and the last 10 000 steps after 10^6 iterations are recorded. Figure 1(b) shows the interdependence of $H(A_n|x_n^i)$ vs ε for $k=30$. The embedding dimension was $m=3$ throughout this work, and was checked by the false nearest neighbor method. Figure 1(b) clearly reveals that the interdependence begins to increase at $\varepsilon_c \approx 0.21$ apparently, indicating a behavior characteristic of a first-order phase transition. At this critical value of coupling, the collective behavior of the system transfers turbulent states into periodic states, as observed in Fig. 1(a). However, Fig. 1(c) uses the method provided by Cisneros *et al.* to quantify the NTCB in the first example. Comparing Figs. 1(b) and 1(c) shows that Fig. 1(c) cannot distinguish clearly

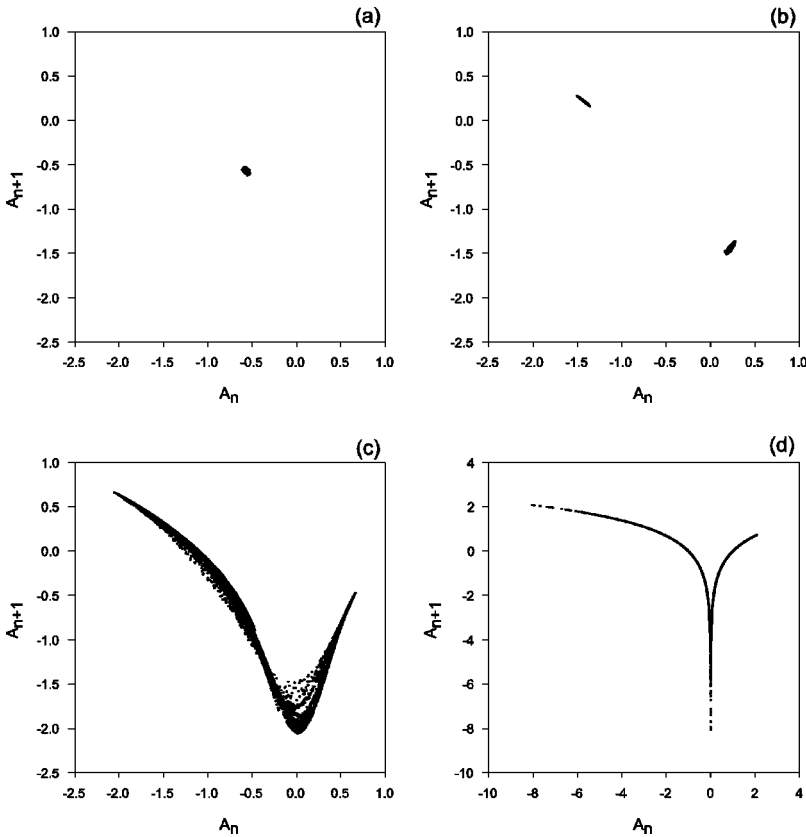


FIG. 2. Return maps A_{n+1} vs A_n of the homogeneous, globally coupled logarithmic maps for different coupling strengths. (a) $\varepsilon=0$ (turbulent phases). (b) $\varepsilon=0.285$ (periodic states). (c) $\varepsilon=0.365$ (chaotic bands). (d) $\varepsilon=0.435$ (chaotic synchronization).

that at which critical coupling strength the nontrivial collective behavior becomes a periodic or synchronous state, but such a value can be distinguished well in Fig. 1(b). Then, $H(A_n|x_n^i)$ gradually decreases to a minimum $\varepsilon \approx 0.365$ and eventually reaches the highest fixed value [after $\varepsilon \approx 0.435$, $S(A_n|x_n^i)$ equals to 1], exceeding the value of periodic states. This phenomenon shows that periodic states become chaotic, then reaching to chaotic synchronization eventually. From the above description, the time series of a single map is sufficient to predict reliably the average state evolution. Accordingly, when the system exhibits periodic states or is undergoing chaotic synchronization, a significant amount of information must flow from the collective dynamics to all elements. The following section will discuss this characteristic.

B. Heterogeneous, globally coupled logarithmic map lattices

This section discusses the heterogeneous, globally coupled-map lattices. Figure 3(a) presents the bifurcation diagram of A_n vs ε for the heterogeneous, globally coupled logarithmic map lattices. In this case, the system size is 10 000 and the local parameter b_i is randomly distributed within a certain range $[-1,1]$. Notably, collective periodic behaviors occur in certain windows of the coupling parameter. Figure 3(b) displays the interdependence $H(A_n|x_n^i)$ vs ε for $k=30$. When $\varepsilon < 0.035$, the interdependence is small unless $\varepsilon_c \approx 0.035$ and then increases continuously for $\varepsilon > \varepsilon_c$. The increase in the interdependence resembles a phase transition from turbulent states to collective periodic states. Fi-

nally, the interdependence begins to decrease, representing the onset of chaotic states.

C. One-dimensional, coupled logarithmic map lattices

The one-dimensional, coupled logarithmic map lattices, as in Eq. (3), also display the nontrivial collective behavior, as presented in Fig. 4(a). The system size is also set to 10 000, and the local dynamics are homogeneous, with $f(x) = b + \ln|x|$, where the local parameter is fixed at $b = -0.8$. In this case, the system represents only a turbulent (statistical fixed point) phase and a period-2 collective state [5]. Figure 4(b) displays $H(A_n|x_n^i)$ vs ε for $k=30$. Again, the interdependence increases where the critical coupling strength value $\varepsilon_c \approx 0.03$, at which the transition occurs from turbulence to periodic collective states, is obtained. Ultimately, the value of interdependence increases to a high value.

D. Homogeneous, globally coupled tent map lattices

The homogeneous, globally coupled tent map lattices with different nontrivial collective behaviors have been discussed. Figure 5(a) illustrates the bifurcation diagram of A_n vs ε and Fig. 6 displays the return maps of A_n for different coupling strengths. The system size is $N = 10\,000$ and the local parameter a is fixed at 1.5 for all maps. For each value of ε , the initial condition is random, and the last 10 000 steps after 10^6 iterations are recorded. As in Sec. III A, four phase areas are

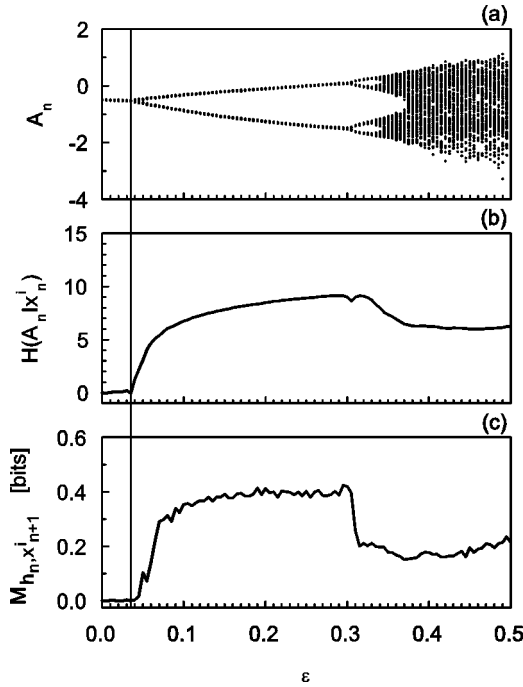


FIG. 3. (a) Bifurcation diagram A_n vs ϵ for heterogeneous, globally coupled logarithmic maps and system size $N=10^4$. (b) $H(A_n|x_n^i)$ vs ϵ for this network. (c) Average information flow M_{h_n, x_{n+1}^i} from h_n to x_{n+1}^i , with $r=0.2$.

also observed: a turbulent phase T [Fig. 6(a)]; collective periodic phases P [Fig. 6(b)]; collective chaotic bands C [Fig. 6(c)]; and chaotic synchronization S [Fig. 6(d)]. The interdependence measure $H(A_n|x_n^i)$, $k=30$, is used to describe the

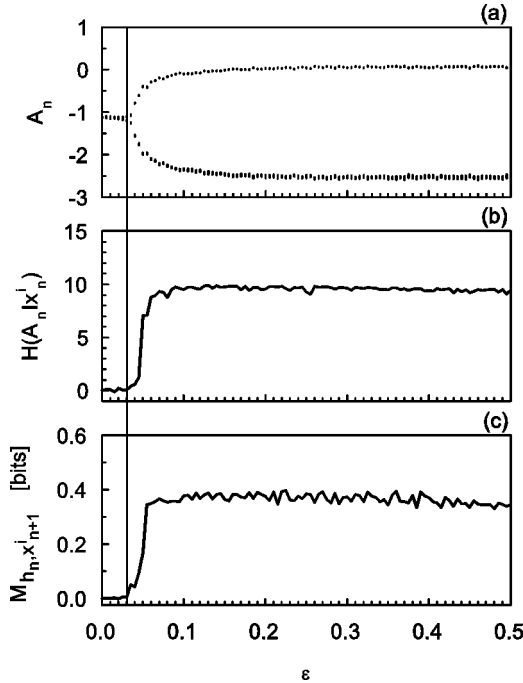


FIG. 4. (a) Bifurcation diagram A_n vs ϵ for one-dimensional, locally coupled logarithmic maps with $b=-0.8$ and system size $N=10^4$. (b) $H(A_n|x_n^i)$ vs ϵ for this lattice. (c) Average information flow M_{h_n, x_{n+1}^i} from h_n to x_{n+1}^i , with $r=0.2$.

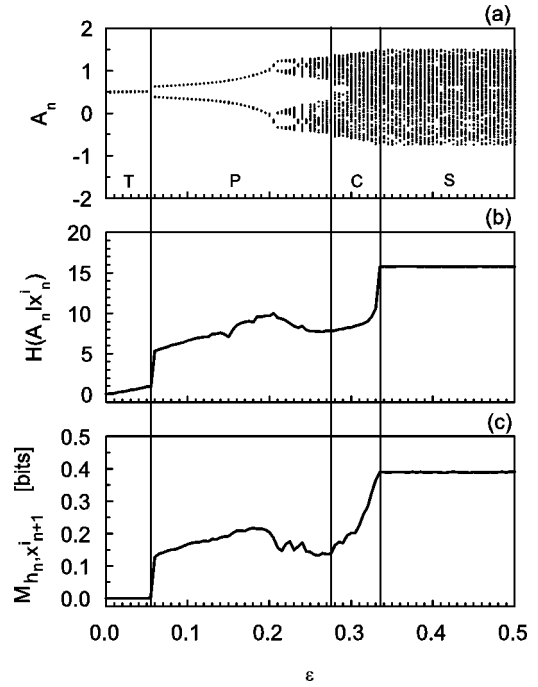


FIG. 5. (a) Bifurcation diagram A_n vs ϵ for homogeneous, globally coupled tent maps and system size $N=10^4$. (b) $H(A_n|x_n^i)$ vs ϵ for this network. (c) Average information flow M_{h_n, x_{n+1}^i} from h_n to x_{n+1}^i , with $r=0.2$.

different behaviors for different coupling strengths [Fig. 5(b)]. After $\epsilon_c \approx 0.055$, the interdependence increases abruptly, indicating that the collective behavior of the system transfers turbulent states more apparently. Then, the interdependence decreases to a minimum $\epsilon \approx 0.275$ and increases to the highest fixed value finally, specifying that the collective behavior of the system has become chaotic, and this leads to chaotic synchronization in the end [after $\epsilon \approx 0.335$ is reached, $S(A_n|x_n^i)$ equals to 1].

As mentioned above, interdependence could be a tool for studying NTCB in chaotic-coupled-map lattices. The following section discusses the relationship between collective behavior and information flow from the mean field h_n to a local map x_{n+1}^i .

IV. INFORMATION FLOW FROM THE MEAN FIELD TO A LOCAL MAP

Numerous authors have used mutual information to quantify the overlap of information contents of two time series. Unfortunately, mutual information includes neither dynamical nor directional information. Consequently, introducing a time delay into one of the observations is important [12]. The basic conceptions of information theory are briefly recalled here. Two time series are assumed to exist, namely, I and J . The mutual information shared by measure i , drawn from a set $I=\{i\}$, and measure j , drawn from a set $J=\{j\}$, is the amount learned by the measure of i about measure j . Expressed in bits, this mutual information is

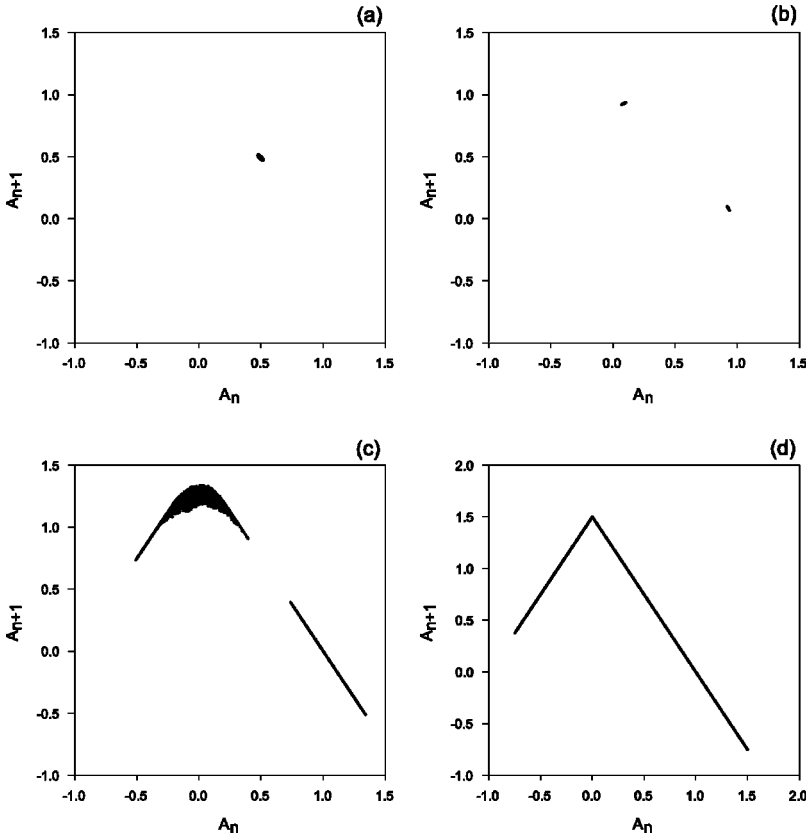


FIG. 6. Return maps A_{n+1} vs A_n of the homogeneous, globally coupled tent maps for different coupling strengths. (a) $\varepsilon=0$ (turbulent phases). (b) $\varepsilon=0.19$ (periodic states). (c) $\varepsilon=0.26$ (chaotic bands). (d) $\varepsilon=0.335$ (chaotic synchronization).

$$\log_2 \frac{p(i,j)}{p(i)p(j)}, \quad (9)$$

where $p(i,j)$ denotes the joint probability density for measures \mathbf{I} and \mathbf{J} , resulting in values i and j . Moreover, $p(i)$ and $p(j)$ are the individual probability densities for the measures of \mathbf{I} and \mathbf{J} . If the measure of a value from \mathbf{I} resulting in i is completely independent of the measure of a value from \mathbf{J} resulting in j , then $p(i,j)$ factorizes to $p(i,j)=p(i)p(j)$. In this case (the amount of information shared by the two measures), namely, the mutual information is zero, as it should be. The average of this information for all measures is called the mutual information between the \mathbf{I} and \mathbf{J} measures, and is expressed as follows:

$$M_{IJ} = \sum_{i,j} p(i,j) \log_2 \frac{p(i,j)}{p(i)p(j)}, \quad (10)$$

which is the well known formula for the mutual information. Here and in the following, the summation index and the subscript of the probabilities specifying the process were omitted. Notably, M_{IJ} is symmetric under the exchange of \mathbf{I} and \mathbf{J} and thus does not contain any directional sense. For this reason, mutual information must be introduced for a time lag in either one of the variables to obtain a directional sense, e.g.,

$$M_{IJ}(\tau) = \sum p(i_n, j_{n-\tau}) \log_2 \frac{p(i_n, j_{n-\tau})}{p(i)p(j)}. \quad (11)$$

The transition probabilities are used here rather than the static probabilities to incorporate the dynamical structure, given by

$$P_r(x_n, y_n) = \frac{1}{N} \sum_{n'} \Theta \left(r - \left| \begin{array}{c} x_n - x_{n'} \\ y_n - y_{n'} \end{array} \right| \right). \quad (12)$$

Moreover, the correlation function $\Theta(x>0)=1$; $\Theta(x\leq 0)=0$ is used. Notably, the norm $|\cdot|$ represents the maximum distance. Different overall scales of \mathbf{I} and \mathbf{J} must be accounted for by using appropriate weights. Dynamically correlated pairs should be excluded as usual. The time-delayed mutual information, with appropriate weights being employed to keep h_n and x_{n+1}^i in the range $[-2, 2]$, is used to obtain information flow from the mean field h_n to a local map x_{n+1}^i . Figure 1(d) presents the average information flow as a function of coupling in the homogeneous, globally coupled-map lattices. Correlation sums at $r=0.2$ were used to calculate the transition probabilities throughout this work, and neighbors closer in time than 100 iterations were excluded from the correlation function. A total of 10 000 iterations of two time series h_n and x_{n+1}^i was recorded after 10^6 steps. A change in the amount of the average information flow from the mean field h_n to a local map x_{n+1}^i can be seen at a critical value of the coupling, $\varepsilon_c \approx 0.21$, which is similar to the interdependence measure. At other coupling strengths, the tendencies are similar to that in Fig. 1(b), and the points of phase transition, such as the straight lines, are matched for both Figs. 1(b) and 1(d). Figure 3(c) plots the average infor-

mation flow vs ε in heterogeneous, globally coupled logarithmic map lattices. The other conditions are the same as in Fig. 1(d). A change in the value of the information flow is observed where coupling $\varepsilon_c \approx 0.035$. Furthermore, once $\varepsilon_c > 0.035$ the values of the average information flow increase continuously and then gradually decrease. This pattern resembles that displayed in Fig. 3(b). Figure 4(c) shows the average information flow as a function of the coupling in the one-dimensional, coupled-map lattices. The pattern displayed in Fig. 4(c) increases continuously after coupling $\varepsilon_c \approx 0.03$ and stays at high values after $\varepsilon_c > 0.03$, as in Fig. 4(b). Finally, Fig. 5(c) plots the average information flow vs ε in homogeneous, globally coupled tent map lattices. Figure 5(c) clearly shows an abrupt increase in the amount of information flow after coupling strength $\varepsilon_c \approx 0.055$, and reaching the highest value eventually after $\varepsilon \approx 0.335$, as in Fig. 5(b). Other tendencies are matched well, such as three straight lines in Fig. 5(b).

From the above, we believe that the change in NTCB must be closely related to the amount of information flow which flows from the instantaneous mean field h_n to a local map x_{n+1}^i .

V. CONCLUSION

This work has applied the interdependence measure to four systems, and has very effectively quantified the non-trivial collective behavior for each coupling. Numerical results indicate that the interdependence measure is better than the method developed by Cisneros *et al.* for definitely differentiating among phase areas. Furthermore, the time-delayed mutual information was used to investigate the amount of information flow from the mean field h_n to a local map x_{n+1}^i . The interdependence measure and the information flow display similar tendencies at every coupling strength, and both increase apparently after each critical coupling ε_c is reached. Therefore, a strong relationship clearly exists between the amount of information flow and the collective system behavior.

ACKNOWLEDGMENT

The authors would like to thank the National Science Council, Taiwan, ROC, for financially supporting this research under Contract No. NSC 91-2112-M-017-002.

-
- [1] *Coupled Map Lattices*, edited by K. Kaneko, special issue of *Chaos* **2**, 279 (1992).
 - [2] H. Chaté and P. Manneville, *Prog. Theor. Phys.* **87**, 1 (1992).
 - [3] L. Cisneros, J. Jiménez, M.G. Cosenza, and A. Parravano, *Phys. Rev. E* **65**, 045204 (2002).
 - [4] H. Chaté and P. Manneville, *Europhys. Lett.* **17**, 291 (1992).
 - [5] M.G. Cosenza, *Phys. Lett. A* **204**, 128 (1995).
 - [6] M.G. Cosenza, *Physica A* **257**, 357 (1998).
 - [7] K. Kaneko, *Phys. Rev. Lett.* **65**, 1391 (1990).
 - [8] A.S. Pikovsky and J. Kurths, *Phys. Rev. Lett.* **72**, 1644 (1994).
 - [9] T. Shibata and K. Kaneko, *Phys. Rev. Lett.* **81**, 4116 (1998).
 - [10] M.G. Cosenza and J. González, *Prog. Theor. Phys.* **100**, 21 (1998).
 - [11] R. Quián Quiroga, J. Arnhold, and P. Grassberger, *Phys. Rev. E* **61**, 5142 (2000).
 - [12] Thomas Schreiber, *Phys. Rev. Lett.* **85**, 461 (2000).
 - [13] Arkady S. Pikovsky and Jürgen Kurths, *Phys. Rev. Lett.* **72**, 1644 (1994).